NIH Public Access
Author Manuscript
Sci Transl Med. Author manuscript; available in PMC 2014 March 14.

Published in final edited form as:
Sci Transl Med. 2012 June 6; 4(137): 137ra73. doi:10.1126/scitranslmed.3003831.

Identification of Naturally Occurring Fatty Acids of the Myelin Sheath That Resolve Neuroinflammation

Peggy P. Ho[1,*], **Jennifer L. Kanter**[1,2,*], **Amanda M. Johnson**[1,2], **Hrishikesh K. Srinagesh**[1], **Eun-Ju Chang**[3,4], **Timothy M. Purdy**[2,3], **Keith P. van Haren**[1,2,3], **William R. Wikoff**[4], **Tobias Kind**[4], **Mohsen Khademi**[5], **Laura Y. Matloff**[1], **Sirisha Narayana**[1,2], **Eun Mi Hur**[1], **Tamsin M. Lindstrom**[2,3], **Zhigang He**[6], **Oliver Fiehn**[4], **Tomas Olsson**[5], **Xianlin Han**[7], **May H. Han**[1], **Lawrence Steinman**[1,†], and **William H. Robinson**[2,3,†]

[1]Department of Neurology and Neurological Sciences, Stanford University School of Medicine, Stanford CA, USA

[2]Division of Immunology and Rheumatology, Department of Medicine, Stanford University School of Medicine, Stanford CA, USA

[3]GRECC, Palo Alto VA Health Care System, Palo Alto CA, USA

[4]Department of Molecular and Cellular Biology and Genome Center, Metabolomics Group, University of California, Davis, Davis, CA USA

[5]Department of Clinical Neuroscience, Karolinska Institute, Stockholm, Sweden

[6]FM Kirby Neurobiology Center, Harvard Medical School, Boston, MA USA

[7]Diabetes and Obesity Research Center, Sanford-Burnham Medical Research Institute, Orlando, FL, USA

Abstract

Lipids comprise 70% of the myelin sheath, and autoantibodies against lipids may contribute to the demyelination that characterizes multiple sclerosis (MS). We used lipid antigen microarrays and lipid mass spectrometry to identify *bona fide* lipid targets of the autoimmune response in MS brain, and an animal model of MS to explore the role of the identified lipids in autoimmune demyelination. We found that autoantibodies in MS target a phosphate group in phosphatidylserine and oxidized phosphatidylcholine derivatives. Administration of these lipids ameliorated experimental autoimmune encephalomyelitis by suppressing activation and inducing apoptosis of autoreactive T cells, effects mediated by the lipids' saturated fatty-acid side chains. Thus, phospholipids represent a natural anti-inflammatory class of compounds that have potential as novel therapeutics for MS.

Correspondence should be addressed to W.H.R. (wrobins@stanford.edu) or L.S. (steinman@stanford.edu).
*/†These authors contributed equally to this work.
P.P.H. and J.L.K., the first authors, and L.S. and W.H.R., the senior authors, contributed equally to this work.

Author contributions: J.L.K., P.P.H., L.S., and W.H.R. formulated the hypothesis and designed the experiments. A.M.J. and S.N.D. contributed to the lipid array studies. P.P.H, J.L.K., A.M.J., H.K.S., and L.Y.M. contributed to the *in vivo* and *in vitro* studies. T.M.P. and K.P.V. also contributed to *in vitro* assays. W.R.W., T.K., O.F., X.H., and M.H.H. contributed to the lipid mass spectrometry studies. P.P.H., E.J.C., and T.M.L. designed and conducted the immunoblotting studies. Z.H. and T.M.L. provided scientific input. M.K., T.O., and M.H.H. provided human samples.

Competing interests: The authors declare no competing interests.

NIH-PA Author Manuscript
NIH-PA Author Manuscript
NIH-PA Author Manuscript

NIH-PA Author Manuscript

NIH-PA Author Manuscript

NIH-PA Author Manuscript

INTRODUCTION

In multiple sclerosis (MS) aberrant adaptive immune responses target and destroy the myelin sheath. Although MS is classically considered a disease driven by T cells, it is now known that autoantibodies also contribute to its pathogenesis (1,2). Several studies on MS demonstrate T-cell and antibody reactivity to lipids (3–6), which comprise over 70% of the myelin sheath. Synthesis of anti-lipid antibodies within the central nervous system (CNS) is associated with an aggressive disease course in MS (7), and, in an experimental model of MS, anti-lipid antibodies both induced demyelination and prevented remyelination (8). Despite recent interest in the potential pathogenicity of antibodies directed against brain lipids, the specificities of the anti-lipid antibody responses in MS remain undefined.

Here we report a “functional lipidomics” approach to discovering autoimmune targets and developing novel therapeutic strategies for MS. We used lipid autoantigen microarrays and lipid mass spectrometry to identify targets of the adaptive autoimmune response in MS patients. We then explored these results in an animal model of MS, experimental autoimmune encephalomyelitis (EAE), in order to define the biological role of the autoantibody-targeted lipids in the pathogenesis of autoimmune demyelination. Unexpectedly, we found that several of the autoantibody-targeted lipids—phospholipids naturally present in the brain —could attenuate EAE. Our findings suggest that phosphatidylserine and oxidized phosphatidylcholine derivatives containing saturated fatty-acid side chains serve as natural brakes on inflammatory responses in the CNS and that this protective mechanism is compromised in MS, as these guardian lipids are attacked by the adaptive arm of the immune system. These naturally occurring myelin lipids may have therapeutic potential in MS and other inflammatory brain diseases.

RESULTS

Anti-lipid-antibody reactivity differentiates between MS patients and controls

We printed lipid antigen arrays containing over 50 brain lipids and used these arrays to profile autoantibodies in cerebrospinal fluid (CSF) samples derived from MS and control patients. An anti-IgG+IgM secondary antibody was used to detect anti-lipid antibody binding. The Significance Analysis of Microarrays (SAM) (9) algorithm identified 17 lipids that had significantly greater reactivity with autoantibodies in CSF from the 33 individuals with MS (18 with relapsing remitting MS [RRMS], 14 with secondary progressive MS [SPMS], and 1 with primary progressive MS [PPMS]) versus the 26 controls (21 with other (non-inflammatory) neurological diseases [OND], and 5 healthy controls [HC]) (false discovery rate [FDR] = 0.048); patient demographics and clinical characteristics are listed in Supplementary Table 1. We used a hierarchical cluster algorithm (10) to discern relationships between patient samples and SAMidentified lipids. Most MS samples clustered together based on the similarity of their anti-lipid autoantibody profiles (Fig. 1A). Specifically, the PPMS sample, and half of the RRMS and SPMS samples, clustered in the group with the highest anti-lipid autoantibody reactivity, whereas only 3 of the 21 OND and none of the HC samples were represented in this group. Most of the controls (15 of 21 OND and 3 of 5 HC) clustered in the group with the lowest anti-lipid autoantibody reactivity, whereas only one SPMS sample and 4 of the 18 RRMS samples clustered in this group. ELISA analysis showed that levels of total IgG were higher than levels of total IgM in both RRMS and OND CSF (Fig. S1A and B), and, as expected, levels of total IgG were significantly higher in RRMS and SPMS CFS than in OND CSF (Fig. S1C).

NIH-PA Author Manuscript

NIH-PA Author Manuscript

NIH-PA Author Manuscript

PGPC reduces EAE severity

To determine whether the autoantibody-targeted lipids have a role in autoimmune demyelination, we tested the effect of select lipids on EAE, a mouse model of MS. In our initial antigen array experiment (Fig. 1A), we screened lipids that fell into 4 categories: 1) brain and myelin lipids, e.g. cerebrosides, sulfatides, and gangliosides; 2) membrane lipids, e.g. cholesterol, phosphatidylcholine, and sphingomyelin; 3) oxidized lipids, e.g. 1-Palmitoyl-2-Glutaroyl-*sn*-Glycero-3-Phosphocholine (PGPC) and its derivatives; and 4) microbial lipids, e.g. LPS and lipoteichoic acid. From our set of 17 lipid hits, we selected several lipids from categories 1–3 that exhibited higher autoantibody reactivity in MS samples than in OND or HC samples. We tested the effects of these lipids in T-cell proliferation assays and in EAE. We found that cerebrosides and gangliosides were unable to suppress $MBP_{Ac1–11}$-specific T-cell proliferation, that administration of cerebrosides or gangliosides did not affect EAE, and that oxidized cholesterol had only a minimal effect on EAE (data not shown). We previously tested sulfatides, which worsened EAE (3).

PGPC, one of the oxidized lipids tested in this screen, was of particular interest because it is a derivative of oxidized phosphatidylcholine, and antibodies to oxidized phosphatidylcholine are present in MS brain lesions (11). Indeed, phosphatidylcholine comprises 30.1% of the lipids in the gray matter and 15.0% of the lipids in the white matter of the adult human brain (12), lipid peroxidation occurs in MS brain lesions (13), and oxidized phosphatidylcholine is present in MS brain lesions (11). We used two treatment regimens to test the effect of exogenous PGPC on EAE. In the first regimen, we subcutaneously administered PGPC together with the proteolipid protein $(PLP)_{139–151}$ that we use to induce EAE in SJL/J mice, and then we intraperitoneally administered PGPC on its own four and seven days after the immunization. In contrast to sulfatide, a myelin glycosphingolipid that exacerbated EAE when delivered in this prophylactic regimen (3), PGPC unexpectedly reduced the severity of EAE throughout the disease course (Fig. 1B and Fig. S2A). In the second regimen, we started administering PGPC 10 days after the immunization, i.e. at the time of disease onset (Fig. S2B), and found that PGPC could also attenuate EAE that was already established. Sphingomyelin composes 6.9% and 7.7% of the lipids in the gray and white matter, respectively, of an adult human brain (12) but exhibited only moderate reactivity to antibodies in MS CSF (Fig. 1A). Sphingomyelin also attenuated EAE when administered during the immunization (Fig. S2A). However, when administered 10 days after the immunization, sphingomyelin exacerbated EAE (Fig. S2B). Thus, unlike the other lipids tested, PGPC attenuated the development of EAE and ameliorated established EAE (Fig. S2).

A reduction in T-cell activation, a process important in MS pathogenesis, accompanied the PGPC-induced attenuation of EAE. The proportion of $CD4^+$ T cells expressing the early activation marker CD69 was reduced among lymph node cells isolated from EAE mice treated prophylactically with PGPC. Specifically, 14.2% of the cells isolated from vehicle-treated mice were $CD4^+CD69^+$, compared to 7.96% of the cells isolated from PGPC-treated mice (Fig. S3A). Moreover, compared to cells from vehicle-treated mice, lymph node cells from PGPC-treated mice proliferated less (Fig. S3B) and splenocytes from PGPC-treated mice secreted less IFN-γ and less TNF (Fig. S3C) upon stimulation with the encephalitogenic $PLP_{139–151}$ peptide.

Phosphocholine head group confers antigenicity

The commonality of the phosphatidylcholine backbone in lipids targeted by autoantibodies in MS prompted us to explore this structure as a potential determinant of antigenicity. We investigated autoantibody targeting of 7 lipids that have a glycero-3-phosphocholine backbone in common with PGPC, as well as targeting of other structurally similar lipids

NIH-PA Author Manuscript

NIH-PA Author Manuscript

NIH-PA Author Manuscript

from the lipid array used in the previous experiments (Fig. 1A)—such as those containing features in common with PGPC, e.g., a phosphate head group with one or two non-polar side chains.

We used Mini Array I, comprising 17 lipids (Supplementary Table 2), to profile autoantibody responses in CSF samples from RRMS patients and OND controls. SAM analysis revealed autoantibody reactivity to 3 of the 7 glycerol-3-phosphocholine-containing lipids (Fig. 2A). All 8 of the lipids identified as targets with the lowest FDR (0.029) had a phosphate group linked to a nitrogen moiety through two carbons (Fig. 2B). The non-polar portion of the targeted lipids contained either one or two side chains; the second side chain in some cases contained a terminal carboxyl group (Fig. 2B). This suggests that autoantibodies present in RRMS CSF target the phospholipids' phosphate head group, and that the affinity of antibody-lipid binding is not specific to a particular phospholipid. In support of this idea, autoantibodies in MS consistently targeted sphingomyelin (3) (Figs. 1A, 2A and B) but did not target ceramide, which is sphingomyelin without the phosphate polar head group (data not shown).

To further investigate the structural basis of the lipids' antigenicity, we examined autoantibody reactivity to an additional 14 lipids that contain various head-group and side-chain modifications of PGPC. The lipids in this Mini Array II are listed in Supplementary Table 2. We probed Mini Array II with CSF samples from RRMS and OND control patients using a sample set similar to that used in the previous array experiments, and identified autoantibody reactivity to many PGPC-related lipids using an anti-IgG secondary antibody (Fig. 2C). We noted that 6 of the 7 targeted lipids had a phosphate group, in most cases attached through two carbons to another polar moiety such as nitrogen or oxygen (Fig. 2D). One such lipid, 1-Palmitoyl-2-Oleoyl-*sn*-Glycerol, contained only a hydroxyl group at this position. Although several of the targeted lipids are endogenously synthesized in human brain, 1,2-dipalmitoyl-sn-glycero-3-phosphocholine (DPPC), a synthetic cationic surfactant that possesses the same head group as PGPC, was also targeted. Of the lipids that were not targeted, 1,2-Dipropionoyl-*sn*-Glycero-3-Phosphocholine (DGPC, right column, 5th lipid) had a phosphate head group with a structure similar to that of the targeted lipids. Unlike the targeted lipids, however, DGPC did not contain long side chains, suggesting that the lipid side chain may also facilitate antibody binding. Despite having only short side chains, DGPC bound to the PVDF membrane on our array (Fig. S4). The other 6 lipids that were not targeted either lacked a phosphate group or contained a phosphate group connected to a bulky group, e.g., a ring structure or a phosphate group linked to 4 carbons (Fig. 2, C and D). Using ELISA analysis to validate our array results, we found that PGPC, 1-hexadecyl-2-azelaoyl-sn-glycero-3-phosphocholine (azPC), 1-Palmitoyl-2-Azelaoyl*sn*-Glycero-3-Phosphocholine (azPC ester), and 1-Palmitoyl-2-Oleoyl-*sn*-Glycero-3-[Phospho-L-Serine] (POPS) are indeed targeted by autoantibodies in CSF, and that the levels of these autoantibodies are significantly higher in CSF from patients with RRMS than in CFS from patients with OND (Fig. S5).

Thus, binding of RRMS CSF autoantibodies to these lipids is dependent on the presence of (i) a non-bulky polar head group such as a phosphate group and (ii) at least one long hydrocarbon side chain.

Antibody targets are natural brain lipids

To determine whether the lipids identified as targets of the autoantibody response (Figs. 1A, 2, S5) are present in MS brain lesions, we performed lipidomic mass spectrometric analysis of pathological specimens taken at autopsy from the brains of MS patients, as previously described (14). Lipids detected in MS brain lesions included phosphatidylcholines, phosphatidylethanolamines, phosphatidylinositols, phosphatidylglycerols,

NIH-PA Author Manuscript

NIH-PA Author Manuscript

NIH-PA Author Manuscript

phosphatidylserines, phosphatidic acids, sphingomyelins, sulfatides, cerebrosides, ceramides, and lysophosphatidylcholines (Supplementary Table 3).

We next asked whether PGPC, azPC, azPC ester, and POPS, specific lipid targets of the autoantibody response in MS (Figs. 1A, 2, S5), are present in MS brain lesions. Mass spectrometric analysis demonstrated the presence of POPS at 0.5–1.3 nmol per mg protein (Fig. 3A and B) in MS brain lesions. Because PGPC, azPC, and azPC ester were not detected in our initial mass spectrometric analysis, we used single reaction monitoring (SRM) to test for the presence of these specific lipids in healthy brain tissue and MS brain lesions. Using SRM, we detected azPC, azPC ester, and PGPC at 5–20 pmol per mg of protein (Fig. 3B). All four lipids were detected both in MS samples and in age-matched control samples, and levels of azPC, azPC ester, PGPC, and POPS were significantly lower in MS samples (Fig. 3B and Supplementary Table 4), consistent with the observed decrease in phosphatidylcholine levels (Supplementary Table 3). We further confirmed the presence of PGPC (Fig. S6), azPC (Fig. S7), and azPC ester (Fig. S8) in human brain extract by liquid chromatography high-resolution mass spectrometry (LC-HRMS), using three criteria: accurate mass agreement with calculated mass (Figs. S6A, S7A, S8A), retention time on the column in comparison to authentic standards (Figs. S6B, S7B, S8B), and MS/MS fragmentation patterns in comparison to authentic standards (Figs. S6C, S7C, S8C).

POPS and oxidized phosphatidylcholine derivatives treat established EAE

Because PGPC attenuated both T-cell proliferation (Fig. S3B) and EAE (Figs. 1B, S2), we performed a second T-cell proliferation screen to determine whether any other oxidized phosphatidylcholine derivatives from our Mini Arrays (Supplementary Table 2) could suppress T-cell proliferation as effectively as PGPC. On the basis of the results from this screen (Fig. S9), we selected the oxidized phosphatidylcholine derivatives azPC and azPC ester, and the phosphatidylserine, POPS, for testing in EAE.

To investigate the therapeutic potential of these autoantibody-targeted lipids in EAE, we administered the initial dose of POPS, PGPC, azPC, or azPC ester to mice with established EAE. We administered the lipids systemically to establish a delivery modality appropriate for future translational studies in humans. The first dose of 100 μg of lipid was injected intravenously into the tail of mice once they developed tail or hind-limb paralysis, and the lipid treatment was repeated every other day, such that 10 injections were administered intravenously during the course of EAE. POPS, PGPC, azPC, and azPC ester were all able to ameliorate established EAE (Fig. 4A).

POPS and oxidized phosphatidylcholine derivatives directly suppress T-cell activity

To investigate the mechanisms by which the autoantibody-targeted lipids provide therapeutic benefit in EAE (Figs. 1B, 4A), we determined whether the lipids could directly inhibit the T-cell-mediated inflammatory responses that underpin EAE. We assessed the effect of these lipids on myelin basic protein $(MBP)_{Ac1–11}$-induced production of cytokines by naïve splenocytes from mice transgenic for the $MBP_{Ac1–11}$-specific T-cell receptor (15). azPC reduced $MBP_{Ac1–11}$-induced T-cell production of the inflammatory cytokines IFN-γ, TNF, and IL-6. POPS also reduced TNF and IL-6 levels but did not significantly reduce IFN-γ levels. PGPC and azPC ester reduced levels of some of the cytokines, but these effects were less dramatic than the effects of POPS or azPC (Fig. 4B). Neither POPS nor the oxidized phosphatidylcholine derivatives affected production of IL-12p40. These lipids had similar inhibitory effects on $PLP_{139–151}$-induced production of IL-17, IL-6, IFN-γ, and TNF by splenocytes from $PLP_{139–151}$-immunized mice (Fig. S10A).

NIH-PA Author Manuscript

NIH-PA Author Manuscript

NIH-PA Author Manuscript

To determine whether the lipids affect T-cell proliferation, we measured ^{3}H-thymidine incorporation in splenocytes stimulated with $MBP_{Ac1–11}$ in the presence of the different lipids. Sulfatide, which worsened EAE, and sphingomyelin, which could not treat established EAE ((3) and Fig. S2B), were used as controls in these assays. POPS, PGPC, azPC, and azPC ester reduced T-cell proliferation in response to $MBP_{Ac1–11}$, whereas sulfatide and sphingomyelin did not (Fig. 4C). We obtained similar results with $PLP_{139–151}$-stimulated splenocytes from mice immunized with $PLP_{139–151}$ (Fig. S10B), as well as with T cells stimulated with anti-CD3 and anti-CD28 antibodies (Fig. S11). Studies using T cells from mice deficient in CD1 showed that the lipid-mediated suppression of T-cell responses occurred through a CD1-independent mechanism (Fig. S11).

POPS and oxidized phosphatidylcholine derivatives induce apoptosis of immune cells

To assess whether programmed cell death contributed to the lipid-mediated reduction in proliferation of activated T cells, we performed Annexin-V staining and 7-amino-actinomycin D (7AAD) uptake assays, which enable identification of early apoptotic (AnnexinV+, 7AAD-) and late apoptotic (AnnexinV+, 7AAD+) cells (Fig. 5A). At 48 hours, azPC ester or PGPC increased T-cell apoptosis 2–3-fold, azPC increased apoptosis >4-fold, and POPS >5-fold. The lipids had differential effects on other cell types, however. azPC and azPC ester suppressed proliferation (Fig. S12A), while only azPC increased apoptosis (Fig. S12B), of a mouse macrophage cell line (RAW 264.7) stimulated with LPS. In contrast, azPC, azPC ester, and POPS modestly suppressed proliferation of purified B cells stimulated with anti-IgM F(ab')2 fragment and anti-CD40 antibodies (Fig. S13A), and only POPS increased apoptosis of the B cells (Fig. S13B).

To determine whether lipid treatment induced apoptosis *in vivo* in the context of EAE, we performed TUNEL staining on sections of brains and spinal cords from EAE mice treated with azPC or POPS. POPS and azPC increased the number of TUNEL-positive cells with lymphocyte morphology in the brain and spinal cord of mice with EAE (Fig. 5C and D).

POPS and oxidized phosphatidylcholine derivatives induce pro-apoptotic and proinflammatory pathways

To investigate the molecular mechanisms underlying the lipid-mediated modulation of T cells, we examined the effects of these lipids on inflammatory, survival, and apoptotic signaling pathways. The transcription factor nuclear factor-kappaB (NF-κB) plays a crucial role in the activation, survival, and proliferation of T cells (16) by driving the transcription of proinflammatory cytokine genes (including *IFN-γ*, *TNF*, and *IL-6* (17–19)), anti-apoptotic genes (20), and genes involved in cell cycle progression (21). Deficiency in NF-κB signaling suppresses the expansion of autoreactive T cells (22). Likewise, extracellular signal-regulated kinase (ERK) activity is integral to cell proliferation and survival (23). Costimulation of T cells with anti-CD3 and anti-CD28 antibodies (CD3/CD28) activated the canonical NF-κB pathway, as indicated by an increase in phosphorylation of the activating kinases IKKα and IKKβ; a decrease in levels of the NF-κB inhibitor IκBα; and an increase in serine 536-phosphorylation of p65, the major transactivating subunit of NF-κB (Fig. 5B). It also induced ERK activity. POPS, PGPC, azPC, and azPC ester each suppressed the CD3/CD28-induced activation of the NF-κB and ERK pathways (Fig. 5B). These lipids also suppressed the CD3/CD28-induced activity (phosphorylation) of B-cell lymphoma protein-2 (Bcl-2) (Fig. 5B), an important anti-apoptotic protein. Bcl-2-interacting molecule (Bim) and Bad, pro-apoptotic members of the Bcl-2 family, antagonize the anti-apoptotic activity of Bcl-2. Importantly, Bim plays critical roles in both activation and apoptosis of autoreactive T cells in EAE (24). ERK-mediated phosphorylation of Bim at serine 69 suppresses the apoptotic activity of Bim (25), while the NF-κB pathway suppresses Bim expression (26,27). Similarly, ERK-mediated phosphorylation of Bad at serine 112 inhibits the

NIH-PA Author Manuscript

NIH-PA Author Manuscript

NIH-PA Author Manuscript

apoptotic activity of Bad (28,29). Collectively, POPS, PGPC, azPC, and azPC ester suppressed the CD3/CD28-induced phosphorylation of Bim and Bad at serines 69 and 112, respectively. Sulfatide, which worsens EAE (3), neither inhibited the NF-κB and ERK pathways, nor suppressed the phosphorylation of the apoptotic Bcl-2 family proteins (Fig. 5B).

Together, these results suggest that suppression of the NF-κB and ERK pathways, and the resulting derepression of apoptotic pathways, underlies the anti-inflammatory and antiproliferative effects of POPS and the oxidized phosphatidylcholine derivatives.

Saturated fatty-acid side chains mediate T-cell suppression

Unsaturated fatty-acid-derived mediators generated in resolving exudates can contribute to the termination of an inflammatory response (30,31). We asked whether the saturated fatty-acid side chains within POPS, PGPC, azPC, and azPC ester could modulate T-cell proliferation and EAE. Fatty acids esterified to the phosphate head group at the *sn*-1 position, and the oxidizable fatty acids at the sn-2 position, were of particular interest in light of their reported roles in modulating inflammation (32). We tested a variety of structural analogs of these fatty-acid side chains, including palmitic acid, ethyl palmitate, sebacic acid, octanoic acid, methyl octanoate, and suberic acid. These molecules form part of the saturated, non-polar side chain of our lipids of interest, which may be cleaved from the phospholipids by lipases that are upregulated in MS brain (14,33). Palmitic acid suppressed T-cell proliferation as effectively as the phospholipids (Fig. 6B); ethyl palmitate, sebacic acid, octanoic acid, methyl octanoate, and suberic acid also suppressed T-cell proliferation, albeit to a lesser extent (data not shown). Palmitic acid also suppressed T-cell production of the inflammatory cytokines IL-6, IL-17, IFN-γ and TNF (Fig. 6C), and induced T-cell apoptosis (Fig. 6D). *In vivo*, administering palmitic acid at the time of disease onset attenuated EAE, and disease relapsed once the palmitic acid treatment was halted (Fig. 6E), indicating that this fatty-acid side chain is itself therapeutically efficacious.

We identified palmitic acid as a fatty-acid side chain present in phosphatidylcholines and as a free, unbound fatty acid in both MS and healthy brain (Supplementary Table 5). Because phospholipases liberate fatty acids from lipids and are upregulated in MS brain (14,33), we tested the effect of azPC on MBP-induced proliferation of T cells pretreated with small-molecule inhibitors of the phospholipases PLC (inhibitor U73122), $cPLA_{2\alpha}$ (EMD525143), $iPLA_2$ (FKGK11), $sPLA_2$ Groups IIA, IID, IIE, V, X (YM 26734), $sPLA_2$ Groups IIA, V (LY 311727), $sPLA_2$ Group V (CAY10590), or $sPLA_2$ Group IIA (EMD525145). We found that pre-incubating T cells with any of the four $sPLA_2$ inhibitors suppressed the effects of azPC (i.e. MBP-stimulated T-cell proliferation was partially restored), whereas pre-incubating the T cells with various concentrations of the other phospholipase inhibitors had no effect or, at high doses, killed the T cells (Fig. S14 and Supplementary Table 6). Together, these results suggest that the non-esterified fatty-acid side chains of the targeted lipids are responsible for their T-cell suppressive properties.

DISCUSSION

We report the use of two lipidomic technologies—lipid antigen arrays and lipidomic mass spectrometry—to identify myelin lipids targeted by autoantibody responses in MS. We show that these autoantibody-targeted phospholipids ameliorate disease in a mouse model of MS by inhibiting the autoaggressive T-cell responses that underpin autoimmune demyelination. Whereas the polar head groups are the lipid components targeted by the autoantibodies, the fatty-acid side chains are the components that mediate the lipids' anti-inflammatory effects. Furthermore, we find that the levels of these autoantibody-targeted lipids are lower in lesions from MS brain than in tissue from healthy brain. Autoantibody targeting may thus

NIH-PA Author Manuscript

NIH-PA Author Manuscript

NIH-PA Author Manuscript

reduce the lipids' anti-inflammatory effect by enhancing their clearance or inhibiting their activity—and thereby compromise the lipid-mediated protection against neuroinflammation.

At the molecular level, the anti-inflammatory effects of the lipids were associated with the inhibition of NF-κB and ERK, signaling molecules that promote inflammation and cell survival, and the derepression of Bim and Bad, the molecular executors of programmed cell death. It is possible that POPS, which contains the phosphoserine moiety detected by 7AAD, could bind and/or integrate into cellular membranes and thereby exaggerate the staining observed with 7AAD. Nevertheless, our observation that POPS induces T-cell apoptosis is confirmed by our *in vivo* results demonstrating increased apoptosis of lymphocytes in the perivascular cuffs of brain and spinal cord lesions of azPC- and POPS-treated mice with EAE. Intriguingly, osteopontin, a protein that induces relapse and progression of EAE, has the opposite effect: it promotes the survival of MBP-reactive T cells by activating the NF-κB pathway and inhibiting Bim-mediated apoptosis (34). Indeed, T-cell apoptosis is a key mechanism by which autoimmune attack on the CNS is kept in check, and it plays an important role in spontaneous EAE remission (35).

In MS brain lesions, inflammation leads to an increase in nitric oxide, which can oxidize lipid components of the brain (36). Using mass spectrometry, we demonstrated the presence of oxidized phospholipids—and specifically of the autoantibody-targeted therapeutic lipids—in normal and in MS brain. We found that levels of oxidized phosphatidylcholine derivatives were lower in MS brain than in healthy brain. This may reflect the autoimmune-mediated destruction of myelin lipids that occurs in MS, such that levels of oxidized phospholipids are diminished despite an increase in lipid peroxidation. The destruction of myelin involves anti-lipid autoantibodies, which can induce demyelination and prevent remyelination in mouse models of MS (8). Through antigen array screening, we found that the CFS of MS patients contains antibodies to oxidized phosphatidylcholine derivatives, and antibodies to oxidized phosphatidylcholine have been detected in MS brain lesions (11), supporting the idea that the antibodies to oxidized phosphatidylcholine derivatives that we detect in CSF can bind their lipid targets in MS brain. Moreover, studies in EAE indicate that antibodies to oxidized phosphatidylcholine are generated as part of the pathological process of autoimmune demyelination (11). Apart from participating in the general destruction of the myelin sheath, such autoantibody targeting of oxidized phosphatidylcholine derivatives could conceivably contribute to MS pathogenesis by reducing the levels or blocking the immunoregulatory activity of these protective lipids.

Oxidized phospholipids are generally considered proinflammatory and may exacerbate inflammation-associated disease (37,38). Whereas oxidized phosphatidylcholine was previously identified as a marker of neuroinflammation in MS (11), our findings suggest that oxidized phosphatidylcholine derivatives in fact function as part of an endogenous feedback mechanism that attenuates adaptive autoimmune responses in the brain. Indeed, oxidized phospholipids are emerging as Janus-like molecules: whereas their pathogenic role in atherosclerosis is well established (32), these lipids play a protective, anti-inflammatory role in endotoxin-induced tissue damage by inhibiting Toll-like receptor-4 signaling (39). Thus, the role of oxidized phospholipids in physiology and pathophysiology is context dependent. In brain, oxidized phosphatidylcholine derivatives and POPS appear to be important mitigators of autoimmune responses.

We find that the saturated, non-polar side chains mediate the protective effects of the therapeutic lipids. Palmitic acid, representative of such fatty-acid side chains present within the lipids, was able to reproduce the therapeutic effects of the lipids *in vitro* and *in vivo*. The results of our inhibitor studies suggest that these fatty acids exert at least some of their immunoregulatory effects following their release from lipids by $sPLA_2$-mediated cleavage.

NIH-PA Author Manuscript

NIH-PA Author Manuscript

NIH-PA Author Manuscript

Levels of $sPLA_2$, and of several other phospholipases, are abnormally high in MS brain lesions (14,40), and $sPLA_2$ plays a key role in the excessive production of arachidonic acid in MS (40). The increase in phospholipase expression in MS brain lesions could increase the levels of anti-inflammatory free fatty acids as part of a feedback mechanism that protects against neuroinflammation. Autoantibody targeting of POPS and oxidized phosphatidylcholine derivatives may compromise this protective feedback mechanism by eliminating the lipids containing the anti-inflammatory fatty acids or by preventing the release of fatty acids from the lipids. Regardless of whether they act as free fatty acids or as phospholipid components, these saturated fatty acids appear to serve a function similar to that of the unsaturated fatty-acid derivatives resolvins and protectins, which mediate resolution of inflammation in tissue exudates (30,31).

The use of lipidomics for drug discovery provides unique opportunities. The adaptive immune system may target molecules that are aberrantly modified or expressed and contribute to the autoimmune pathology (41). However, our results suggest that the immune system may also drive autoimmune disease by abrogating the protective effects of molecules involved in inflammatory homeostasis. Choosing the target of the antibody as a potential therapeutic, in this case the lipids identified on an autoantibody array, provides a fresh strategy for screening putative therapeutics. We found that the phosphocholine head group is an important determinant of the antigenicity of brain lipids, a discovery that enabled the identification of additional therapeutic lipids through stringent statistical analysis of lipid microarray data combined with lipidomic mass spectrometric analysis. The identification of lipids targeted by autoantibodies affords the opportunity to mine small lipid-soluble molecules as potential new drugs for autoimmune disease.

MATERIALS AND METHODS

Reagents

We obtained POPS, PGPC, sphingomyelin, sulfatide, azPC, azPC ester, and all other phosphatidylcholine derivatives listed in Supplementary Table 2 from Avanti Polar Lipids. Palmitic acid was purchased from Sigma. Proteolipid protein $(PLP)_{139–151}$ (HCLGKWLGHPDKF) and $MBP_{Ac1–11}$(ASQKRPSQRHG)were synthesized and HPLC-purified (>97%) by the Stanford PAN facility.

Patient CSF samples

All human samples were collected and used under protocols approved by the Institutional Review Boards of the Karolinska Institute and Stanford University. Patient demographics and clinical characteristics are listed in Supplementary Table 1.

Lipid array analysis

Lipid arrays were generated and analyzed as previously described (3). Briefly, we used a Camag Automatic TLC Sampler 4 robot to print 10 to 100 pmol of lipids on PVDF membranes affixed to the surface of microscope slides. These lipid arrays were probed with 1:20 dilutions of human CSF, followed by 1:8000 dilutions of either anti-human IgG+IgM or anti-human IgG (Jackson Immunoresearch) conjugated to horseradish peroxidase (HRP). Bound HRP-conjugated antibodies were visualized by chemiluminescence (ECL Plus, Amersham) and autoradiography. We used GenePix Pro 5.0 software (Molecular Devices) to extract the net median pixel intensities for individual features from digital images of the array autoradiographs. We applied the SAM (9) algorithm (version 1.21) to identify lipids with statistically significant differences in array reactivity between groups of humans or mice. The list of ‘significant lipids’ with the lowest q value (false discovery rate, FDR) is

NIH-PA Author Manuscript

NIH-PA Author Manuscript

NIH-PA Author Manuscript

reported in each heatmap Figure. We arranged the SAM results into relationships by using Cluster software and displayed the results by using TreeView software (10).

Lipidomic analysis of brain samples

Archived postmortem samples from MS brain and age-matched healthy brain were analyzed by shotgun lipidomics as previously described (42–44) and as outlined in the Supplementary Methods. The six MS brain samples analysed were as follows: MS 1, an active lesion from a 59-year-old female with relapsing-remitting MS; MS 2, an active lesion from a 72-year-old male with secondary progressive MS; MS 3, a chronic active lesion from a 47-year-old female with chronic MS; MS 4, a chronic active lesion from a 76-year-old male with chronic MS; MS 5, an acute active lesion from a 31-year-old female in the relapsing phase of relapsing-remitting MS; MS 6, a chronic active lesion from the same 31-year-old female with relapsing-remitting MS. Control brain samples were thoroughly examined to rule out the presence of neurological disease. Control samples were obtained from normal-appearing white matter from the brains of the following individuals: C1, 23-year-old male; C2, 52-year-old female; C3, 23-year-old male; C4, 52-year-old male; C5, 82-year-old male; and C6, 44-year-old female. Samples of healthy brain and samples of MS lesions were pulverized in liquid nitrogen. Lipid extracts were generated and analysed by electrospray ionization mass spectrometry (typically within 1 week) using a TSQ Quantum Ultra Plus triple-quadrupole mass spectrometer (Thermo Fisher Scientific) equipped with an automated nanospray apparatus (Nanomate HD, Advion Bioscience Ltd.) and Xcalibur system software (45).

EAE induction

Animal experiments were approved by, and performed in compliance with, the National Institute of Health guidelines of the Institutional Animal Care and Use Committee at Stanford University. For induction of EAE, 8- to 12-week-old female SJL/J mice (Jackson Laboratory) were immunized subcutaneously with 100 μg of $PLP_{139–151}$ emulsified in CFA (Difco Laboratories). *Lipid co-immunization:* Three injections of PGPC (6 μg/mouse/injection) or vehicle (0.05% Tween-20 in PBS) were delivered on days 0, 4, and 7 after immunization with $PLP_{139–151}$. On day 0, the lipid or vehicle was emulsified together with $PLP_{139–151}$ in CFA and administered by subcutaneous injection. At subsequent time points, lipid or vehicle was injected intraperitoneally. EAE was assessed as previously described (3). *Lipid and palmitic-acid treatment:* Administration of lipid, palmitic acid, or vehicle was initiated once the $PLP_{139–151}$-immunized mice developed paralysis (representing clinical EAE) and repeated every other day, for a total of ten separate injections. 100 μg of POPS, PGPC, azPC ester, azPC, palmitic acid, or vehicle (0.05% Tween-20 in PBS) was administered in 0.2 ml intravenously in the tail.

Proliferation and cytokine assays

Splenocytes were harvested from mice transgenic for the $MBP_{Ac1–11}$-specific T-cell receptor (15) and stimulated with 2 μg/ml of $MBP_{Ac1–11}$ in the presence of 30 μg/ml of lipid. Lymph nodes and spleens were also harvested from naive C57BL/6 mice, and $CD3^+$ T-cell enrichment columns (R&D systems) were used to isolate $CD3^+$ T cells. The purified $CD3^+$ T cells were stimulated with 5 μg/ml of plate-bound anti-CD3 antibodies and anti-CD28 antibodies in the presence of 30 μg/ml of POPS, PGPC, azPC ester, brain sulfatides, or azPC, 0.25 mM palmitic acid, or 100% ethanol (as the vehicle control). For assessment of proliferation, 1 μCi of ^3H-thymidine was added to each well for the final 18–24 hours of culture, and incorporation of radioactivity was measured by using a Betaplate scintillation counter. Cytokine assays were performed on culture supernatants after 24 (IL-12p40) or 48 hours (IFN-γ, IL-6, IL-17A and TNF) of culture by using the BD OptEIA™ Mouse ELISA kits (BD Biosciences) or Mouse IL-17 DuoSet ELISA Development kit (R&D Systems).

NIH-PA Author Manuscript

NIH-PA Author Manuscript

NIH-PA Author Manuscript

Flow cytometry

Cells were stained according to standard protocols, run on a FACScan flow cytometer (BD Biosciences), and analysed with CellQuest software (BD Immunocytometry Systems). The antibody conjugate used was FITC anti-CD4, clone GK1.5 (BDPharmingen). 7AAD staining was performed by using the Annexin V-PE Apoptosis Detection Kit I (BD Pharmingen).

Western blotting

$CD3^+$ T cells were isolated from the lymph nodes of naïve C57BL/6 mice by using $CD3^+$ T-cell enrichment columns (R&D systems). T cells were pre-incubated with 30 μg/ml of lipid for 1 hour at 37 °C degrees and then stimulated with plate-bound anti-CD3 and anti-CD28 antibodies (5 μg/ml, eBiosciences) in the presence of the lipids for 15 minutes or 24 hours. Cells were washed with ice-cold PBS and lysed in RIPA lysis buffer containing 1× Halt protease and phosphatase inhibitor cocktail (Pierce) with a Dounce homogenizer. Immunoblotting was performed with antibodies against phospho-Bim (serine 69), phospho-Bad (serine 112), phospho-Bcl-2 (serine 70), phospho-IKKα/β (serines 180/181), phospho-p65 (serine 536), phospho-ERK1/2 (threonine 202/tyrosine 204), and IκBα from Cell Signaling Technology.

TUNEL assay

Mice with EAE were treated intravenously with 200 μg of azPC, 200 μg of POPS, or vehicle (0.05% Tween-20 in PBS) on day 15 after immunization with CFA and $PLP_{139–151}$ peptide. Mice were treated with lipids for 12, 24, or 48 hours and then sacrificed and perfused with 4% paraformaldehyde. Brains and spinal cords were embedded in paraffin and sectioned. TUNEL-positive cells were detected by using the In Situ Cell Death Kit, AP (Roche) according to the manufacturer's instructions.

Supplementary Material

Refer to Web version on PubMed Central for supplementary material.

Acknowledgments

This work was funded by the National Institutes of Health and the Department of Veterans Affairs to W.H.R.; the National Institutes of Health to L.S.; a National Multiple Sclerosis Society Paul, Hastings, Janofsky & Walker Postdoctoral Fellowship to J.L.K.; and the National Institute on Aging to X.H.

REFERENCES

1. Genain CP, Cannella B, Hauser SL, Raine CS. Identification of autoantibodies associated with myelin damage in multiple sclerosis. Nat Med. 1999; 5:170–175. [PubMed: 9930864]
2. Goverman J. Autoimmune T cell responses in the central nervous system. Nat Rev Immunol. 2009
3. Kanter JL, Narayana S, Ho PP, Catz I, Warren KG, Sobel RA, Steinman L, Robinson WH. Lipid microarrays identify key mediators of autoimmune brain inflammation. Nat Med. 2006; 12:138–143. [PubMed: 16341241]
4. Pender MP, Csurhes PA, Wolfe NP, Hooper KD, Good MF, McCombe PA, Greer JM. Increased circulating T cell reactivity to GM3 and GQ1b gangliosides in primary progressive multiple sclerosis. J Clin Neurosci. 2003; 10:63–66. [PubMed: 12464524]
5. Quintana FJ, Farez MF, Viglietta V, Iglesias AH, Merbl Y, Izquierdo G, Lucas M, Basso AS, Khoury SJ, Lucchinetti CF, Cohen IR, Weiner HL. Antigen microarrays identify unique serum autoantibody signatures in clinical and pathologic subtypes of multiple sclerosis. Proc Natl Acad Sci U S A. 2008; 105:18889–18894. [PubMed: 19028871]

NIH-PA Author Manuscript NIH-PA Author Manuscript NIH-PA Author Manuscript

6. Shamshiev A, Donda A, Carena I, Mori L, Kappos L, De Libero G. Self glycolipids as T-cell autoantigens. Eur J Immunol. 1999; 29:1667–1675. [PubMed: 10359121]
7. Villar LM, Sadaba MC, Roldan E, Masjuan J, Gonzalez-Porque P, Villarrubia N, Espino M, Garcia-Trujillo JA, Bootello A, Alvarez-Cermeno JC. Intrathecal synthesis of oligoclonal IgM against myelin lipids predicts an aggressive disease course in MS. J Clin Invest. 2005; 115:187–194. [PubMed: 15630459]
8. Rosenbluth J, Schiff R, Liang WL, Dou W. Antibody-mediated CNS demyelination II. Focal spinal cord lesions induced by implantation of an IgM antisulfatide-secreting hybridoma. J Neurocytol. 2003; 32:265–276. [PubMed: 14724389]
9. Tusher VG, Tibshirani R, Chu G. Significance analysis of microarrays applied to the ionizing radiation response. Proc Natl Acad Sci U S A. 2001; 98:5116–5121. [PubMed: 11309499]
10. Eisen MB, Spellman PT, Brown PO, Botstein D. Cluster analysis and display of genome-wide expression patterns. Proc Natl Acad Sci U S A. 1998; 95:14863–14868. [PubMed: 9843981]
11. Qin J, Goswami R, Balabanov R, Dawson G. Oxidized phosphatidylcholine is a marker for neuroinflammation in multiple sclerosis brain. J Neurosci Res. 2007; 85:977–984. [PubMed: 17304573]
12. Agranoff, BW.; Benjamins, JA.; Hajra, AK. Lipids. In: Siegel, GJ.; Agranoff, BW.; Albers, RW.; Fisher, SK.; Uhler, MD., editors. Basic Neurochemistry: Molecular, Cellular and Medical Aspects. Philadelphia: Lippincott-Raven Publishers; 1999.
13. van Horssen J, Schreibelt G, Drexhage J, Hazes T, Dijkstra CD, van der Valk P, de Vries HE. Severe oxidative damage in multiple sclerosis lesions coincides with enhanced antioxidant enzyme expression. Free Radic Biol Med. 2008; 45:1729–1737. [PubMed: 18930811]
14. Han MH, Hwang SI, Roy DB, Lundgren DH, Price JV, Ousman SS, Fernald GH, Gerlitz B, Robinson WH, Baranzini SE, Grinnell BW, Raine CS, Sobel RA, Han DK, Steinman L. Proteomic analysis of active multiple sclerosis lesions reveals therapeutic targets. Nature. 2008; 451:1076–1081. [PubMed: 18278032]
15. Lafaille JJ, Nagashima K, Katsuki M, Tonegawa S. High incidence of spontaneous autoimmune encephalomyelitis in immunodeficient anti-myelin basic protein T cell receptor transgenic mice. Cell. 1994; 78:399–408. [PubMed: 7520367]
16. Schulze-Luehrmann J, Ghosh S. Antigen-receptor signaling to nuclear factor kappa B. Immunity. 2006; 25:701–715. [PubMed: 17098202]
17. Collart MA, Baeuerle P, Vassalli P. Regulation of tumor necrosis factor alpha transcription in macrophages: involvement of four kappa B-like motifs and of constitutive and inducible forms of NF-kappa B. Mol Cell Biol. 1990; 10:1498–1506. [PubMed: 2181276]
18. Libermann TA, Baltimore D. Activation of interleukin-6 gene expression through the NF-kappa B transcription factor. Mol Cell Biol. 1990; 10:2327–2334. [PubMed: 2183031]
19. Sica A, Dorman L, Viggiano V, Cippitelli M, Ghosh P, Rice N, Young HA. Interaction of NF-kappaB and NFAT with the interferon-gamma promoter. J Biol Chem. 1997; 272:30412–30420. [PubMed: 9374532]
20. Dutta J, Fan Y, Gupta N, Fan G, Gelinas C. Current insights into the regulation of programmed cell death by NF-kappaB. Oncogene. 2006; 25:6800–6816. [PubMed: 17072329]
21. Hinz M, Krappmann D, Eichten A, Heder A, Scheidereit C, Strauss M. NF-kappaB function in growth control: regulation of cyclin D1 expression and G0/G1-to-S-phase transition. Mol Cell Biol. 1999; 19:2690–2698. [PubMed: 10082535]
22. Greve B, Weissert R, Hamdi N, Bettelli E, Sobel RA, Coyle A, Kuchroo VK, Rajewsky K, Schmidt-Supprian M. I kappa B kinase 2/beta deficiency controls expansion of autoreactive T cells and suppresses experimental autoimmune encephalomyelitis. J Immunol. 2007; 179:179–185. [PubMed: 17579036]
23. Anjum R, Blenis J. The RSK family of kinases: emerging roles in cellular signalling. Nat Rev Mol Cell Biol. 2008; 9:747–758. [PubMed: 18813292]
24. Ludwinski MW, Sun J, Hilliard B, Gong S, Xue F, Carmody RJ, Devirgiliis J, Chen YH. Critical roles of Bim in T cell activation and T cell-mediated autoimmune inflammation in mice. J Clin Invest. 2009

NIH-PA Author Manuscript NIH-PA Author Manuscript NIH-PA Author Manuscript

25. Luciano F, Jacquel A, Colosetti P, Herrant M, Cagnol S, Pages G, Auberger P. Phosphorylation of Bim-EL by Erk1/2 on serine 69 promotes its degradation via the proteasome pathway and regulates its proapoptotic function. Oncogene. 2003; 22:6785–6793. [PubMed: 14555991]
26. Essafi A, Fernandez de Mattos S, Hassen YA, Soeiro I, Mufti GJ, Thomas NS, Medema RH, Lam EW. Direct transcriptional regulation of Bim by FoxO3a mediates STI571-induced apoptosis in Bcr-Abl-expressing cells. Oncogene. 2005; 24:2317–2329. [PubMed: 15688014]
27. Hu MC, Lee DF, Xia W, Golfman LS, Ou-Yang F, Yang JY, Zou Y, Bao S, Hanada N, Saso H, Kobayashi R, Hung MC. IkappaB kinase promotes tumorigenesis through inhibition of forkhead FOXO3a. Cell. 2004; 117:225–237. [PubMed: 15084260]
28. Bonni A, Brunet A, West AE, Datta SR, Takasu MA, Greenberg ME. Cell survival promoted by the Ras-MAPK signaling pathway by transcription-dependent and -independent mechanisms. Science. 1999; 286:1358–1362. [PubMed: 10558990]
29. Zha J, Harada H, Yang E, Jockel J, Korsmeyer SJ. Serine phosphorylation of death agonist BAD in response to survival factor results in binding to 14-3-3 not BCL-X(L). Cell. 1996; 87:619–628. [PubMed: 8929531]
30. Haworth O, Cernadas M, Yang R, Serhan CN, Levy BD. Resolvin E1 regulates interleukin 23, interferon-gamma and lipoxin A4 to promote the resolution of allergic airway inflammation. Nat Immunol. 2008; 9:873–879. [PubMed: 18568027]
31. Schwab JM, Chiang N, Arita M, Serhan CN. Resolvin E1 and protectin D1 activate inflammation-resolution programmes. Nature. 2007; 447:869–874. [PubMed: 17568749]
32. Fruhwirth GO, Loidl A, Hermetter A. Oxidized phospholipids: from molecular properties to disease. Biochim Biophys Acta. 2007; 1772:718–736. [PubMed: 17570293]
33. Lock C, Hermans G, Pedotti R, Brendolan A, Schadt E, Garren H, Langer-Gould A, Strober S, Cannella B, Allard J, Klonowski P, Austin A, Lad N, Kaminski N, Galli SJ, Oksenberg JR, Raine CS, Heller R, Steinman L. Gene-microarray analysis of multiple sclerosis lesions yields new targets validated in autoimmune encephalomyelitis. Nat Med. 2002; 8:500–508. [PubMed: 11984595]
34. Hur EM, Youssef S, Haws ME, Zhang SY, Sobel RA, Steinman L. Osteopontin-induced relapse and progression of autoimmune brain disease through enhanced survival of activated T cells. Nat Immunol. 2007; 8:74–83. [PubMed: 17143274]
35. Pender MP. Treating autoimmune demyelination by augmenting lymphocyte apoptosis in the central nervous system. J Neuroimmunol. 2007; 191:26–38. [PubMed: 17931708]
36. Bagasra O, Michaels FH, Zheng YM, Bobroski LE, Spitsin SV, Fu ZF, Tawadros R, Koprowski H. Activation of the inducible form of nitric oxide synthase in the brains of patients with multiple sclerosis. Proc Natl Acad Sci U S A. 1995; 92:12041–12045. [PubMed: 8618840]
37. Barton M, Minotti R, Haas E. Inflammation and atherosclerosis. Circ Res. 2007; 101:750–751. [PubMed: 17932331]
38. Berliner JA, Subbanagounder G, Leitinger N, Watson AD, Vora D. Evidence for a role of phospholipid oxidation products in atherogenesis. Trends Cardiovasc Med. 2001; 11:142–147. [PubMed: 11686004]
39. Bochkov VN, Mechtcheriakova D, Lucerna M, Huber J, Malli R, Graier WF, Hofer E, Binder BR, Leitinger N. Oxidized phospholipids stimulate tissue factor expression in human endothelial cells via activation of ERK/EGR-1 and Ca(++)/NFAT. Blood. 2002; 99:199–206. [PubMed: 11756172]
40. Cunningham TJ, Yao L, Oetinger M, Cort L, Blankenhorn EP, Greenstein JI. Secreted phospholipase A2 activity in experimental autoimmune encephalomyelitis and multiple sclerosis. Journal of neuroinflammation. 2006; 3:26. [PubMed: 16965627]
41. Klareskog L, Ronnelid J, Lundberg K, Padyukov L, Alfredsson L. Immunity to citrullinated proteins in rheumatoid arthritis. Annu Rev Immunol. 2008; 26:651–675. [PubMed: 18173373]
42. Cheng H, Jiang X, Han X. Alterations in lipid homeostasis of mouse dorsal root ganglia induced by apolipoprotein E deficiency: a shotgun lipidomics study. J Neurochem. 2007; 101:57–76. [PubMed: 17241120]
43. Han X, Gross RW. Shotgun lipidomics: multidimensional MS analysis of cellular lipidomes. Expert Rev Proteomics. 2005; 2:253–264. [PubMed: 15892569]

NIH-PA Author Manuscript

NIH-PA Author Manuscript

NIH-PA Author Manuscript

44. Han X, Gross RW. Shotgun lipidomics: electrospray ionization mass spectrometric analysis and quantitation of cellular lipidomes directly from crude extracts of biological samples. Mass Spectrom Rev. 2005; 24:367–412. [PubMed: 15389848]

45. Han X, Yang K, Gross RW. Microfluidics-based electrospray ionization enhances the intrasource separation of lipid classes and extends identification of individual molecular species through multi-dimensional mass spectrometry: development of an automated high-throughput platform for shotgun lipidomics. Rapid Commun Mass Spectrom. 2008; 22:2115–2124. [PubMed: 18523984]

NIH-PA Author Manuscript

NIH-PA Author Manuscript

NIH-PA Author Manuscript

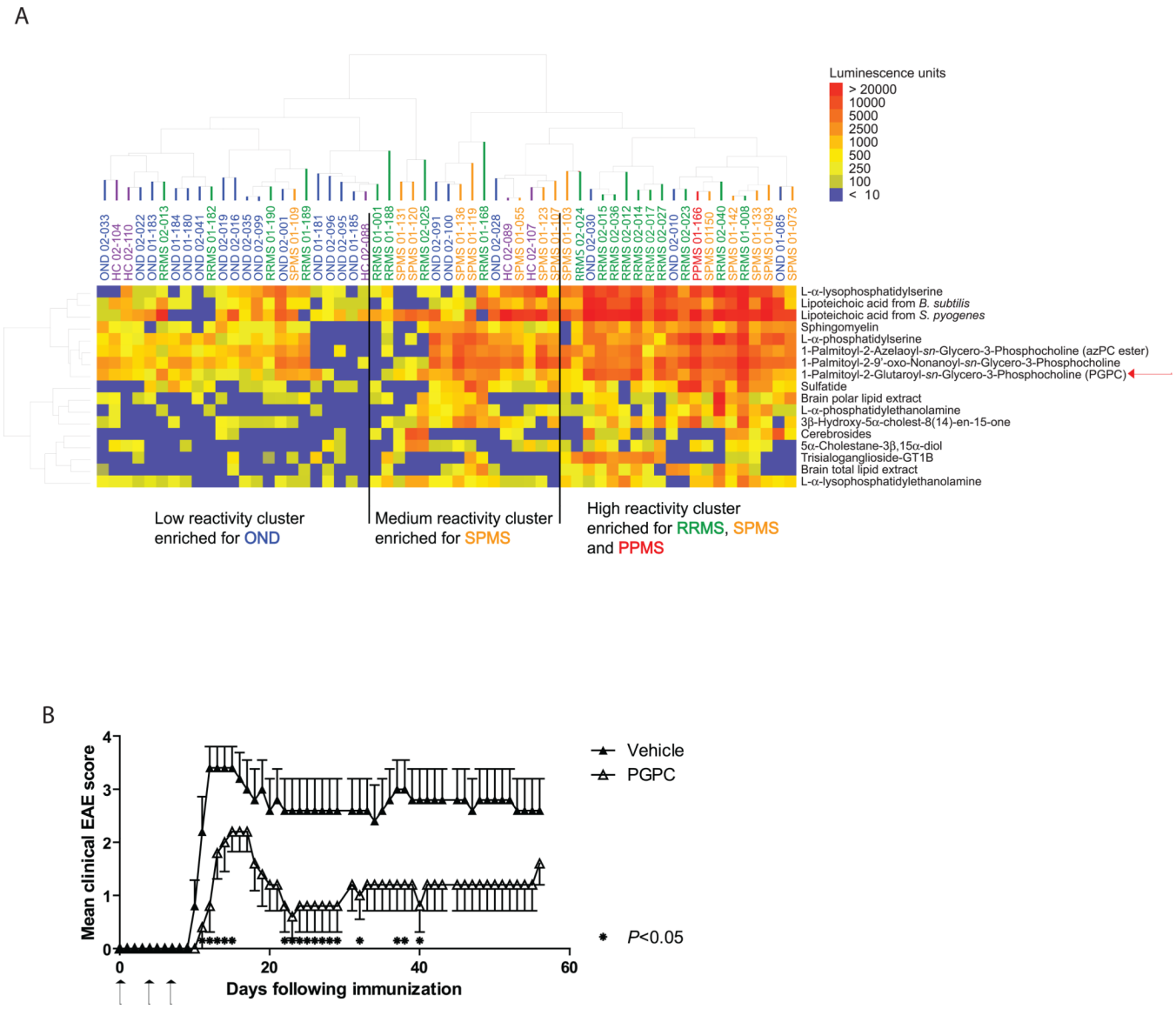

Fig. 1.

Autoantibody targeting of lipids is higher in MS CSF than in OND CSF and normal CSF, and the autoantibody-targeted lipid PGPC attenuates EAE. (**A**) Lipid-array profiling of IgG +IgM antibody reactivity in CSF samples from MS patients (RRMS, relapsing remitting MS; SPMS, secondary progressive MS; PPMS, primary progressive MS), healthy controls (HC), and other neurological disease (OND) controls. Lipid hits with the lowest FDR (q=0.048) were clustered according to their reactivity profiles. Sample type and ID number are shown above the heatmap, and the lipids targeted are shown to the right of the heatmap. The patients' demographics and clinical characteristics are presented in Supplementary Table 1. (**B**) Clinical EAE scores of mice coinjected subcutaneoulsy with $PLP_{139–151}$ and 6 μg/injection of PGPC (day 0); on days 4 and 7 after immunization, PGPC was injected intraperitoneally. Arrows indicate when PGPC was administered. Each point represents the mean ± SEM, and results are representative of 4 independent experiments. **P* < 0.05 Mann-Whitney test, vehicle control (*n* = 5) vs PGPC (*n* = 5).

NIH-PA Author Manuscript
NIH-PA Author Manuscript
NIH-PA Author Manuscript

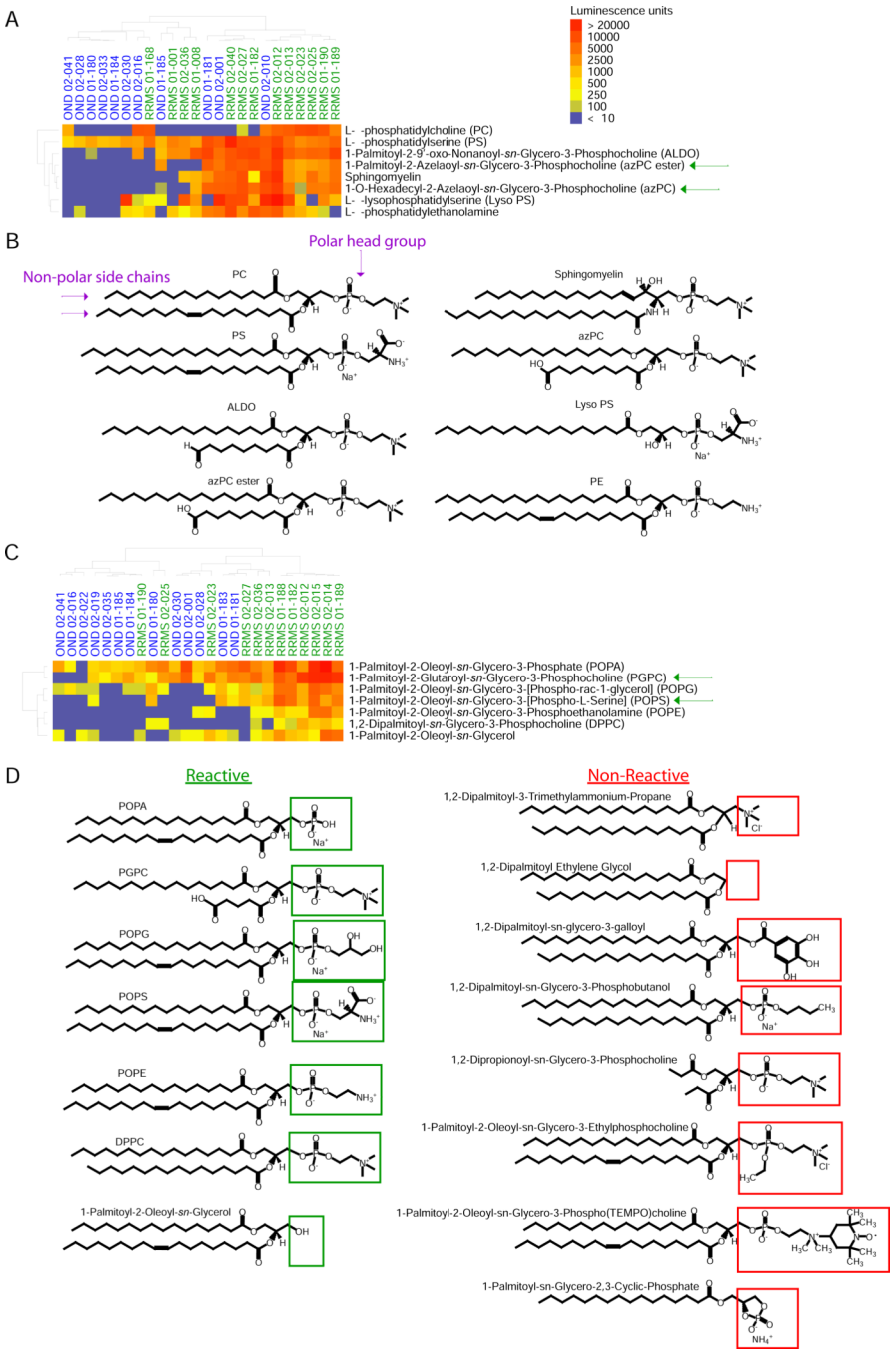

Fig. 2.

PGPC-related lipids with non-bulky polar head groups are targeted by antibodies in CSF of MS patients. (**A**) Mini-Array I: IgG antibody reactivity to various glycero-3-phosphocholine lipids in CSF samples from patients with relapsing remitting MS (RRMS) and from control patients with other neurological disease (OND). Lipid hits with the lowest FDR (q=0.029) were clustered according to their reactivity profiles. Sample type and ID number are shown above the heatmap, and the lipids targeted are shown to the right of the heatmap. (**B**) Structures of lipid hits in (A). (**C**) Mini-Array II: IgG antibody reactivity to lipids constituting polar head-group and side-chain modifications of PGPC in CSF samples from

RRMS patients and OND controls. Lipid hits with the lowest FDR (q=0.016) were clustered according to their reactivity profiles. All of the lipids screened in Mini Array I and II are listed in Supplementary Table 2. (**D**) Left column, structures of the lipid targets identified in (C), with green boxes around the polar head group; right column, structures of the lipids that were not targeted, with red boxes around the polar head group.

NIH-PA Author Manuscript
NIH-PA Author Manuscript
NIH-PA Author Manuscript

NIH-PA Author Manuscript
NIH-PA Author Manuscript
NIH-PA Author Manuscript

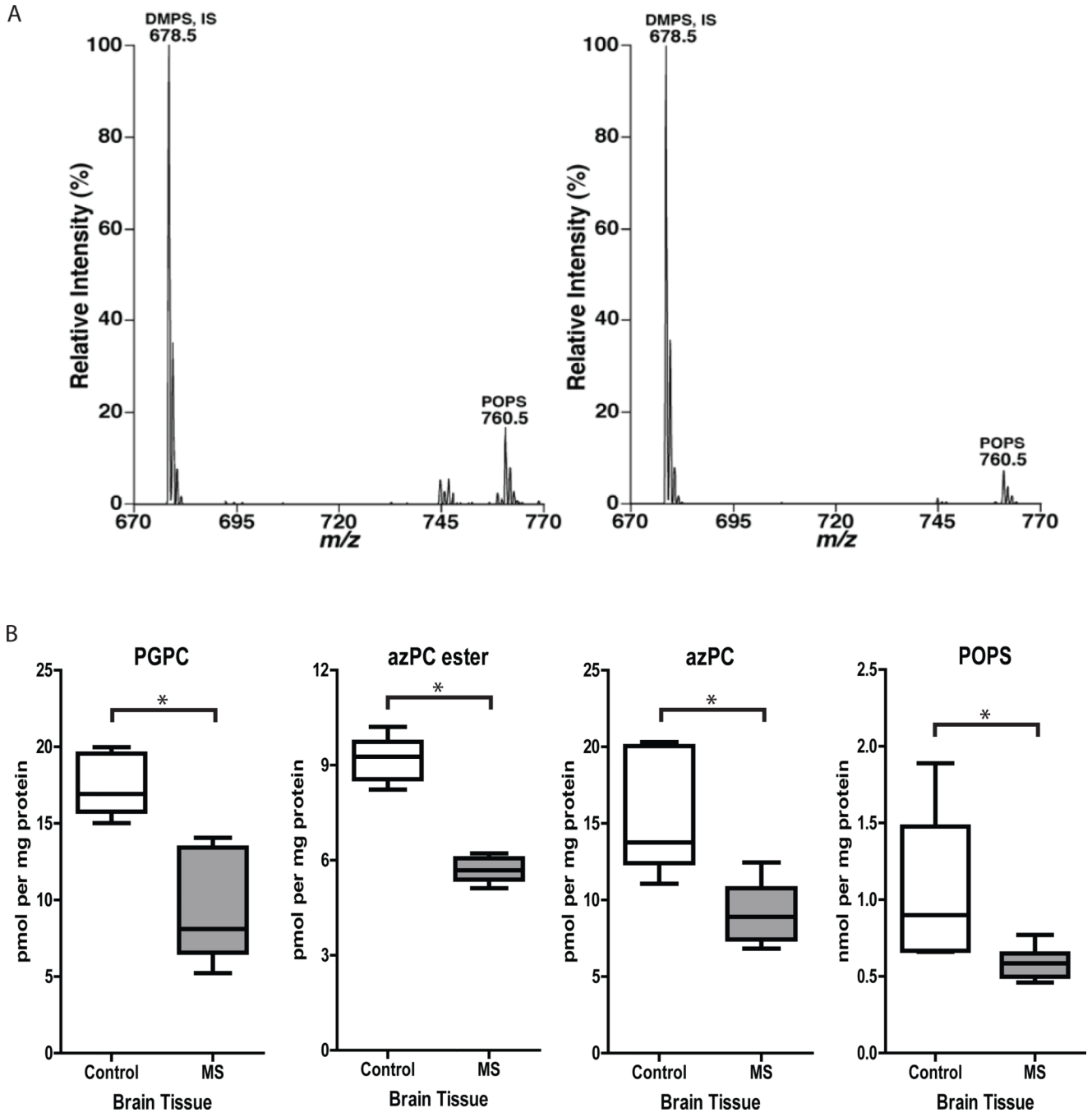

Fig. 3.

Levels of POPS, PGPC, azPC, and azPC ester are higher in MS brain than in healthy brain. (**A**) Negative-ion electrospray ionization mass spectrometric analyses of palmitoyl oleoyl phosphatidylserine (POPS) in lipid extracts of normal-appearing white matter from an age-matched healthy control brain (left panel) and of an active lesion from a brain afflicted with relapsing remitting MS (right panel). DMPS, dimyristoryl phosphatidylserine; IS, internal standard. (**B**) Single-reaction monitoring analysis of PGPC azPC ester, azPC, and POPS levels in samples of MS brain lesions ($n = 6$) and healthy brain tissue ($n = 6$). Controls: age-matched individuals with no signs of neurological disease; MS: 3 patients with relapsing

remitting MS; 1 patient with secondary progressive MS; and 2 patients with chronic MS. *$P<0.05$ by unpaired Student's *t*-test.

NIH-PA Author Manuscript
NIH-PA Author Manuscript
NIH-PA Author Manuscript

NIH-PA Author Manuscript

NIH-PA Author Manuscript

NIH-PA Author Manuscript

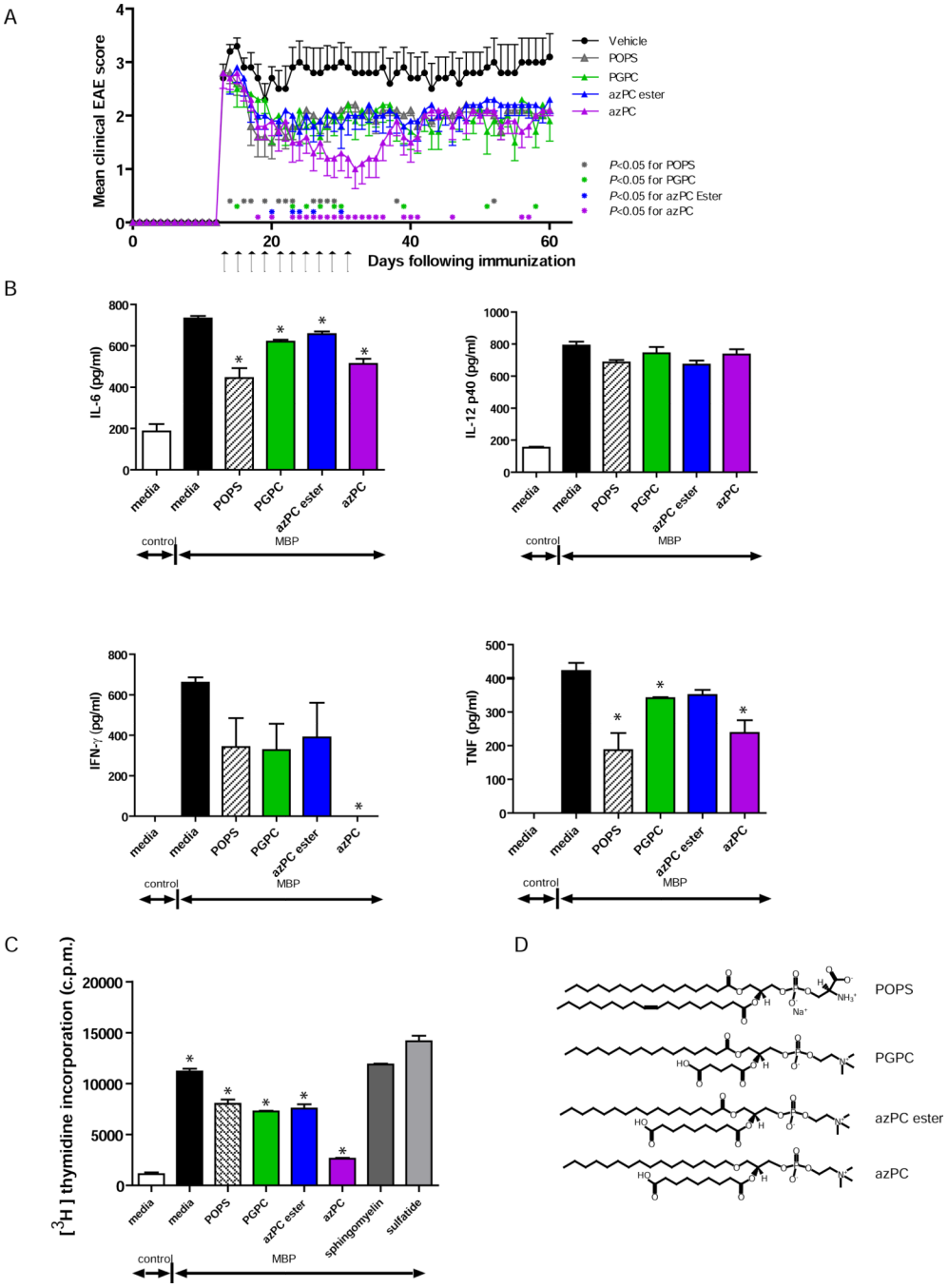

Fig. 4.

Administration of lipids that are targeted by autoantibodies and whose levels are decreased in MS attenuate ongoing EAE and T-cell activation. (**A**) Clinical scores of $PLP_{139–151}$-immunized SJL mice treated at the peak of EAE with 100 μg/injection of POPS (n = 10), PGPC (n = 10), azPC ester (n = 10), azPC (n = 10), or vehicle alone (n = 10). Arrows indicate injections of lipid or vehicle. Each point represents the mean clinical score ± SEM (* denotes time points at which $P < 0.05$ by Mann-Whitney test comparing vehicle treatment vs. lipid treatment). (**B**) Cytokine production by and (**C**) proliferation of naive $MBP_{Ac1–11}$-TCR transgenic splenocytes stimulated with 2 μg/ml $MBP_{Ac1–11}$ in the presence of 30 μg/ml

of lipid (structures shown in **D**), as indicated. Values are the mean + SEM of triplicates. Results are representative of 3 independent experiments. *$P < 0.05$ by Student's *t*-test, each lipid plus $MBP_{Ac1–11}$ vs. $MBP_{Ac1–11}$ alone.

NIH-PA Author Manuscript
NIH-PA Author Manuscript
NIH-PA Author Manuscript

NIH-PA Author Manuscript
NIH-PA Author Manuscript
NIH-PA Author Manuscript

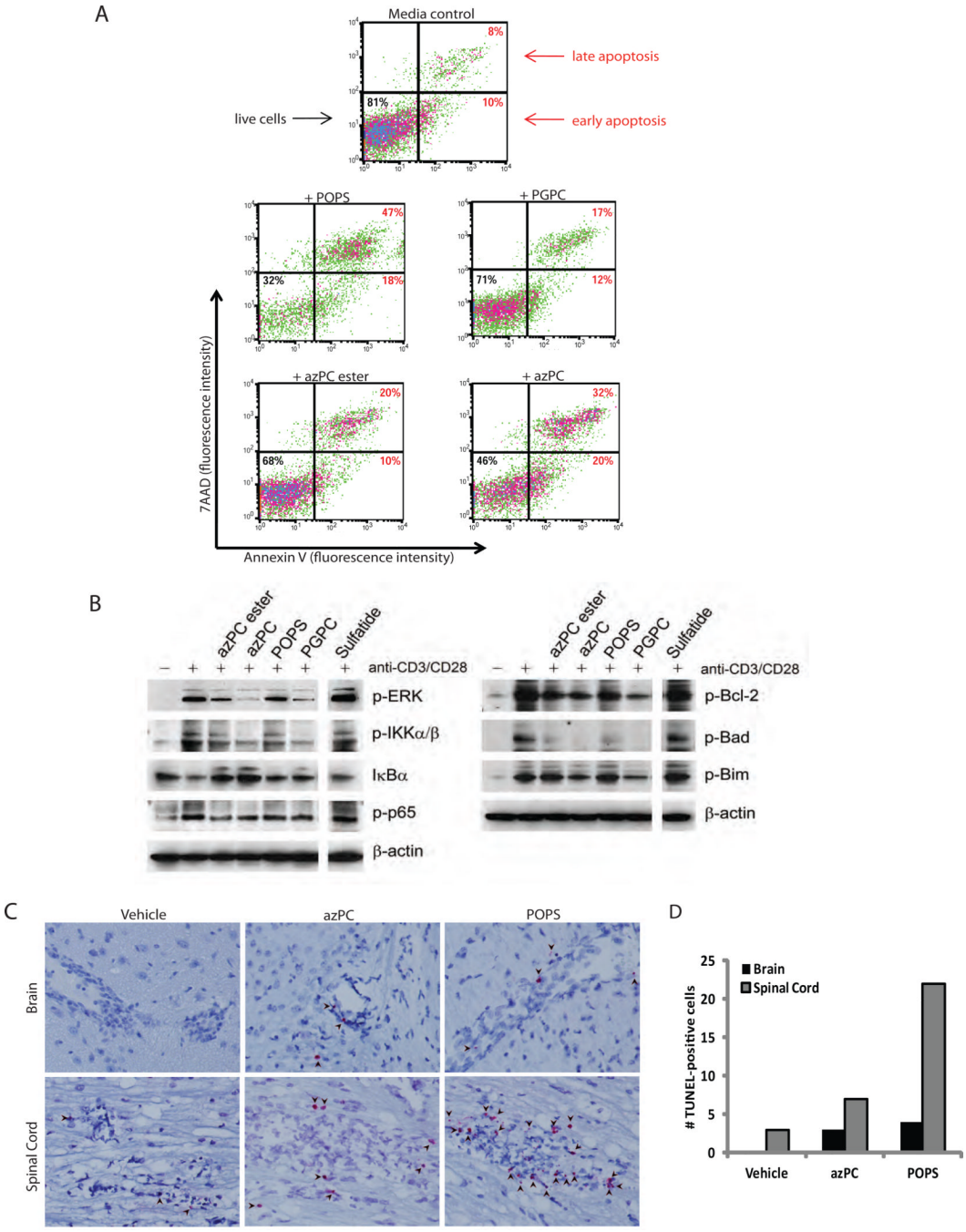

Fig. 5.

POPS, PGPC, azPC, and azPC ester induce apoptotic signaling pathways and T-cell apoptosis. (**A**) Annexin V and 7AAD staining of $CD3^+$ T cells purified from wild-type B6 mice and stimulated with plate-bound anti-CD3 and anti-CD28 antibodies for 48 h with or without 30 μg/ml of lipid. Cells are gated on $CD4^+$ T cells, and results are representative of 3 experiments. (**B**) Immunoblot analysis of phopsho-ERK1/2, phospho-IKKα/β, phospho-p65, IκBα, phospho-Bcl-2, phospho-Bad, and phospho-Bim in lysates of wild-type $CD3^+$ T cells stimulated with plate-bound anti-CD3 and anti-CD28 antibodies for 15 min (left panel) and 24 h (right panel) in the presence of 30 μg/ml of lipid, as indicated. Blots are

representative of two independent experiments. (**C**) TUNEL staining of brain and spinal-cord tissue from mice immunized with $PLP_{139–151}$ peptide (to induce EAE) and treated for 12 h with azPC, POPS, or vehicle on day 15 after immunization. Arrows indicate TUNEL-positive (bright pink/red) infiltrating cells in the perivascular cuffs of lesions from mice with active EAE. Original magnification, ×400. (D) Quantification of TUNEL-positive infiltrating cells in brain and spinal cord sections shown in panel (C).

NIH-PA Author Manuscript
NIH-PA Author Manuscript
NIH-PA Author Manuscript

NIH-PA Author Manuscript
NIH-PA Author Manuscript
NIH-PA Author Manuscript

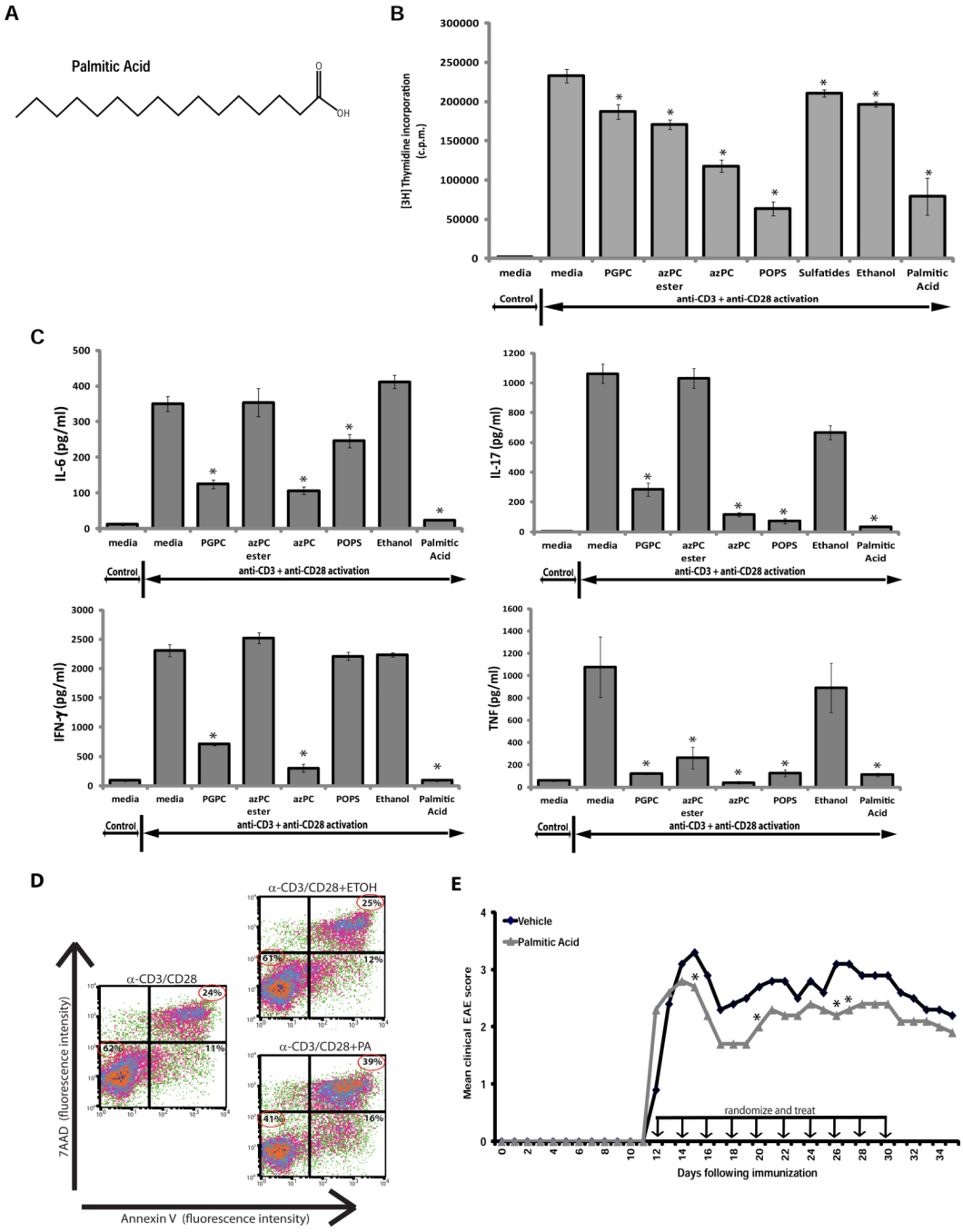

Fig. 6.

Palmitic acid, a non-polar side chain of 1-Palmitoyl phospholipids, suppresses T-cell proliferation and inflammatory cytokine production, induces T-cell apoptosis, and attenuates EAE. (**A**) Structure of palmitic acid. (**B**) Proliferation and (**C**) cytokine production of naive T cells purified from wild-type B6 mice and stimulated for 48 h with 5 μg/ml of anti-CD3 and anti-CD28 antibody and either 30 μg/ml of lipid or 0.25 mM of palmitic acid. Values are the mean + s.e.m. of triplicates. Results are representative of 3 independent experiments (*$P < 0.05$ by Student's *t*-test, compared to anti-CD3/anti-CD28 alone). (**D**) Apoptosis (indicated by annexin V and 7AAD staining) of $CD3^+$ T cells purified from wild-type B6

NIH-PA Author Manuscript

NIH-PA Author Manuscript

NIH-PA Author Manuscript

mice and stimulated with plate-bound anti-CD3 and anti-CD28 antibodies for 48 h alone or with ethanol (ETOH) or 0.25 mM of palmitic acid (PA). Cells are gated on $CD4^+$ T cells. (**E**) Clinical scores of $PLP_{139–151}$-immunized SJL mice treated at the peak of EAE with 100 μg/injection of palmitic acid ($n = 10$), or vehicle alone ($n = 10$). Arrows indicate injections of palmitic acid or vehicle. Each point represents the mean clinical score (*$P < 0.05$ by Mann-Whitney test comparing vehicle treatment vs. palmitic acid treatment).